Molecules and Cells

# Chromatin Interacting Factor OsVIL2 Is Required for Outgrowth of Axillary Buds in Rice

Jinmi Yoon[1], Lae-Hyeon Cho[1,2], Sichul Lee[3], Richa Pasriga[1], Win Tun[1], Jungil Yang[1], Hyeryung Yoon[1], Hee Joong Jeong[1], Jong-Seong Jeon[1], and Gynheung An[1,*]

[1]Graduate School of Biotechnology and Crop Biotech Institute, Kyung Hee University, Yongin 17104, Korea, [2]Department of Plant Bioscience, Pusan National University, Miryang 50463, Korea, [3]Center for Plant Aging Research, Institute for Basic Science, Daegu 42988, Korea
*Correspondence: genean@khu.ac.kr
https://doi.org/10.14348/molcells.2019.0141
www.molcells.org

**Shoot branching is an essential agronomic trait that impacts on plant architecture and yield. Shoot branching is determined by two independent steps: axillary meristem formation and axillary bud outgrowth. Although several genes and regulatory mechanism have been studied with respect to shoot branching, the roles of chromatin-remodeling factors in the developmental process have not been reported in rice. We previously identified a chromatin-remodeling factor OsVIL2 that controls the trimethylation of histone H3 lysine 27 (H3K27me3) at target genes. In this study, we report that loss-of-function mutants in *OsVIL2* showed a phenotype of reduced tiller number in rice. The reduction was due to a defect in axillary bud (tiller) outgrowth rather than axillary meristem initiation. Analysis of the expression patterns of the tiller-related genes revealed that expression of *OsTB1*, which is a negative regulator of bud outgrowth, was increased in *osvil2* mutants. Chromatin immunoprecipitation assays showed that OsVIL2 binds to the promoter region of *OsTB1* chromatin in wild-type rice, but the binding was not observed in *osvil2* mutants. Tiller number of double mutant *osvil2 ostb1* was similar to that of *ostb1*, suggesting that *osvil2* is epistatic to *ostb1*. These observations indicate that OsVIL2 suppresses *OsTB1* expression by chromatin modification, thereby inducing bud outgrowth.**

**Keywords:** bud outgrowth, chromatin modification, rice

## INTRODUCTION

Shoot branching is one of the critical agronomic traits, contributing to biomass and grain yield in crops (Tian and Jiao, 2015). Rice tillers are specialized shoot branches that are formed on the unelongated basal internode and grow independently from the main culm (Li et al., 2003). Rice tillering affects panicle development such as the number of primary and secondary branches, so that branching determines grain number per panicle (Wang and Li, 2011).

Tillers arise from the axillary bud apical meristem (AM), which develops in the axils of leaves during the vegetative stage in rice (Wang and Li, 2011). The development of tillers undergoes two processes: formation of the axillary bud and outgrowth of the axillary (tiller) bud (Wang and Li, 2011). At Stage 1, the AM consists of cytoplasm-dense cells which form as a bulge in the axil of the leaf primordium. The bulge develops into a cone-like structure at Stage 2. The dome and prophylls become gradually more evident at Stage 3, and the axillary bud is formed at Stage 4 (Tanaka et al., 2015).

In rice, *Oryza sativa homeobox1* (*OSH1*), which is preferentially expressed in the AM, is required for the initiation of AM formation and the maintenance of undifferentiated cell

Received 25 June, 2019; revised 17 October, 2019; accepted 29 October, 2019; published online 27 November, 2019

eISSN: 0219-1032

fate (Tanaka et al., 2015). *LAX PANICLE1* (*LAX1*) also plays an essential role in AM formation by genetically functioning together with *LAX PANICLE2* (*LAX2*) and *MONOCULM1* (*MOC1*) (Tabuchi et al., 2011). *LAX1* is expressed in the leaf axil at Stage 4 and the transcription factor accumulates to a high level in two to three layers of cells in the boundary region between the axillary bud and the shoot AM (SAM). Although differentiation of the meristematic cells is initiated in *lax1* mutants, AM formation is defective (Oikawa and Kyozuka, 2009).

*TILLERS ABSENT1* (*TAB1*; *OsWUS*) encodes a transcriptional regulator containing a homeodomain WUS box and an ethylene-responsive element-binding factor (EAR) motif and is expressed in the pre-meristem zone. Mutation of *TAB1* causes reduction in *OSH1* expression in the pre-meristematic region and defects in AM formation (Tanaka et al., 2015). Another factor involved in AM formation is a *LEAFY* ortholog, *RICE FLORICULA/LEAFY* (*RFL*), also called *ABERRANT PANICLE ORGANIZATION 2* (*APO2*) (Deshpande et al., 2015). *RFL* is preferentially expressed in the axils of leaves at the juvenile vegetative stage and maintains AM specification by promoting expression of *LAX1* and *CUP SHAPED COTYLEDON* (*CUC*) genes (Deshpande et al., 2015).

Not all of the axillary buds develop immediately into tillers and some of them stay dormant until maturity. Final tiller number depends mainly on the capability of axillary bud outgrowth (Wai and An, 2017; Wang and Li, 2011), which is affected by various environmental factors and hormones (Deshpande et al., 2015).

Auxins and cytokinins influence the outgrowth of tiller buds (Wai and An, 2017). Auxins are synthesized at the shoot apex and transported by the polar auxin transport system. In rice, a polar auxin transporter, OsPIN1, is essential for auxin-dependent tiller bud emergence. Reduction of *OsPIN1* gene expression causes an increase in tiller number due to the disturbance of auxin-dependent tiller bud inhibition (Xu et al., 2005). Similarly, *OsPIN2* also controls tiller number (Chen et al., 2012). Another auxin transporter gene *OsPIN3* appears to be involved in tiller development because expression of this gene is reduced in the culm of *RFL* knock-down plants (Deshpande et al., 2015). Expression of auxin-responsive genes such as *OsIAA7* and *OsIAA20* is also affected in *RFL* knock-down plants (Deshpande et al., 2015). Endogenous cytokinins in axillary buds are considered to act as activators of axillary bud outgrowth (Yeh et al., 2015). In rice, Cytokinin Oxidase2 (OsCKX2), which is an enzyme which degrades cytokinins, inhibits shoot branching by reducing endogenous cytokinin levels (Yeh et al., 2015).

Strigolactone (SL), a carotenoid phytohormone, suppresses axillary bud outgrowth (Wang et al., 2013). Rice mutants defective in the biosynthesis or signaling of SLs display increased branching phenotypes (Wai and An, 2017; Zhang et al., 2010; Zhao et al., 2014; Zou et al., 2006). *DWARF10* (*D10*), encoding carotenoid cleavage dioxygenase 8, is involved in inducing axillary bud outgrowth by reducing auxin levels and transport (Zhang et al., 2010). *HIGH-TILLERING DWARF1* (*HDT1*), encoding carotenoid cleavage dioxygenase 7, also stimulates the outgrowth of axillary buds (Zou et al., 2006). A SL-biosynthesis gene, *DWARF27* (*D27*), is predominantly expressed in axillary buds and inhibits outgrowth of tiller buds (Lin et al., 2009), whereas *DWARF3* (*D3*), encoding a nuclear-localized F-box protein, inhibits the outgrowth of axillary buds by forming a Skp, Cullin, F-box containing (SCF) complex with DWARF14 (D14) and DWARF53, that are involved in SL signaling (Ishikawa et al., 2005; Jiang et al., 2013; Nakamura et al., 2013).

Several transcription factors control outgrowth of axillary buds. Rice *TEOSINTE BRANCHED1* (*OsTB1*) is a negative regulator of the outgrowth of axillary buds, while *OsMADS57* is a positive factor controlling tiller outgrowth (Guo et al., 2013; Minakuchi et al., 2010). Loss-of-function of *OsTB1* causes thin culms and excessive tillering, while overexpression of the gene results in reduced tillering (Minakuchi et al., 2010; Takeda et al., 2003). OsTB1 interacts with OsMADS57 to repress expression of *D14*, a gene involved in SL signaling, to regulate axillary bud outgrowth; OsMADS57 affects tiller outgrowth by suppressing the expression of *D14*. This negative regulation by OsMADS57 is inhibited by physical interaction with OsTB1 to make balancing of *D14* expression for tiller outgrowth (Guo et al., 2013).

Although many of the chromatin-remodeling factors are found to control plant development such as flowering time and panicle architecture in rice, their roles in shoot branching have not been studied. Polycomb repressive complex 2 (PRC2), which represses target gene expression by regulating the trimethylation of histone 3 lysine 27 (H3K27me3) of the chromatin of the target gene, plays essential roles as an epigenetic repressor (Mozgova and Henning, 2015). The rice VERNALIZATION INSENSITIVE 3-like (VIL3) protein OsVIL2 associates with the PRC2 complex to suppress target gene expression by mediating H3K27me3 (Yang et al., 2013; 2019). The *osvil2* null mutants exhibit pleiotropic phenotypes including alteration of leaf angle, reduced tiller number, floral organ defects, and a change in flowering time (Yang et al., 2013; Yoon et al., 2018). In the current study, we demonstrate that OsVIL2 induces tillering by controlling the chromatin state of *OsTB1*.

## MATERIALS AND METHODS

### Plant materials and growth condition

We previously reported the T-DNA null mutants, *osvil2-1* and *osvil2-2*, that were isolated from a T-DNA-tagged line pool in *Oryza sativa japonica* cv. Dongjin (Jeon et al., 2000; Jeong et al., 2002; Yang et al., 2013). We have previously generated transgenic plants carrying the *OsVIL2* promoter-*GUS* construct (Yang et al., 2013; 2019; Yoon et al., 2018). Plants were grown in a growth room under long-day conditions (14-h light at 28°C/10-h dark at 23°C).

### RNA extraction and reverse transcription-polymerase chain reaction (RT-PCR) analysis

The cDNAs were synthesized from 2 μg of total RNA isolated from basal parts of the shoots using RNAiso Plus (Takara, Japan). Moloney murine leukemia virus reverse transcriptase (Promega, USA), RNasin Ribonuclease Inhibitor (Promega), 10 ng of oligo (dTs) and 2.5 mM deoxiribonucleotide triphosphates were included in the reaction mixture. Quantitative

RT-PCR (RT-qPCR) was performed with a Rotor-Gene 6000 (Corbett Research, Australia) using SYBR Green I Prime Q-Mastermix (GeNet Bio, Korea) as described previously (Cho et al., 2016; 2018b). The internal control was *OsUbi1*. The ΔΔCT method was used to calculate levels of relative expression (Yoon et al., 2014). Primers used in this study are presented in Supplementary Table 1.

### Histochemical analysis and GUS assay

Basal parts of the seedlings were fixed in a formaldehyde-acetic acid-alcohol solution at 4°C. Samples were dehydrated with an ethanol series, treated with a tert-butyl alcohol and infiltrated with paraffin. After embedding, samples were cut into 10-μm thick slices with a microtome (Leica Microsystems, Germany). Slices were stained with toluidine blue and observed under a BX61 microscope (Olympus, Japan) as previously reported (Yoon et al., 2017). For GUS staining, samples were incubated in a GUS staining solution containing and 0.1% X-gluc (5-bromo-4-chloro-3-indolyl-β-D-glucuronic acid, cyclohexylammonium salt), 5% methanol, 2% dimethyl sulfoxide (DMSO), 100 mM sodium phosphate (pH 7.0), 5 mM potassium ferricyanide, 5 mM potassium ferrocyanide, 0.5% Triton X-100, and 10 mM EDTA (pH 8.0) (Yoon et al., 2017). Chlorophylls were removed from the stained samples by immersion in 70% ethanol for 2 h and in 95% ethanol overnight at 65°C.

### *In situ* RNA hybridization

To prepare the RNA probe, a gene-specific fragment was amplified by PCR and cloned in pBluescript II. Digoxigenin (DIG)-labeled sense and antisense RNA probes were prepared as previously reported (Lee and An, 2012; Lee et al., 2007; Yoon et al., 2014). RNA *in situ* hybridization was performed as previously reported (Lee and An, 2012; Lee et al., 2007; Yoon et al., 2014). Briefly, samples were fixed in 4% paraformaldehyde solution. After dehydration, the paraffin block was infiltrated, and sectioned. Slices from the samples were rehydrated and incubated in a solution containing the DIG-labeled RNA probe overnight at 57°C. The slices were treated with anti-DIG alkaline phosphatase (Roche Molecular Biochemicals, Germany) and stained with nitroblue tetrazolium chloride/5-bromo-4-chloro-3-indolyl phosphate (NBT/BCIP).

### Chromatin immunoprecipitation (ChIP) assay

Basal parts of at least 10 plants at 28 days after germination (DAG) were harvested for the assay. ChIP was performed as previously reported (Haring et al., 2007). For cross-linking, 1-g samples were incubated with 3% formaldehyde solution. After nuclei were isolated, chromatin was sheared to approximately 500- to 1,000-bp length by sonication. Anti-trimethyl-histone H3 (Lys27) monoclonal antibody was used for immunoprecipitation (07-449; Millipore, USA) (Yang et al., 2019). For normalization, we used the fold enrichment method in which the values obtained from the antibody reaction were divided by values from no-antibody controls (Haring et al., 2007). The primers for this analysis are listed in Supplementary Table 2.

### Plasmid vector construction

Plasmid vector for *osvil2 ostb1* double mutant was constructed by the polycistronic tRNA-gRNA (PTG)/Cas9 method (Xie et al., 2015). The plasmid pRGEB32 was used for *Agrobacterium*-mediated rice transformation. The pGTR plasmid, which contains a gRNA-tRNA fused fragment, was used as a template to synthesize PTGs. Primers are listed in Supplementary Table 3.

### Statistical analyses

The data were analyzed by one-way ANOVA, with pairwise multiple comparison tests carried out by the Tukey honestly significant difference test to compare samples, using the R program (Cohen and Cohen, 2008).

## RESULTS

### Mutations in *OsVIL2* cause a reduction in tiller development

To determine whether tiller development is dependent on flowering time in rice, we studied tiller phenotypes of various flowering mutants that we had generated in *japonica* varieties Hwayoung and Dongjin. In general, late-flowering mutants produced more tillers, whereas early-flowering mutants had fewer tillers. However, *osvil2* mutants exhibited phenotypes which flowered approximately 4 weeks later than the wild-type (WT) (Fig. 1A) and had a reduced tiller number (Fig. 1B).

Neither *osvil2* mutants nor WT plants produced axillary tillers at 14 DAG (Figs. 1B and 1C). WT plants started to develop axillary tillers at 21 DAG, while *osvil2* mutants did not produce tillers at that stage (Figs. 1B and 1D). WT continued to develop new tillers reaching a total of approximately six per plant, and no new tillers were actively produced after 63 DAG (Figs. 1B, 1E, and 1F). Because floral signals Hd3a and RFT1 start to be generated at approximately 63 DAG (Cho et al., 2018a; 2018b), these signals appear to suppress new tiller generation. In contrast to WT plants, *osvil2* mutant plants produced only one axillary tiller at 42 to 56 DAG, and no further tiller development was observed subsequently (Figs. 1B, 1E, and 1F). This observation indicated that OsVIL2 promoted axillary tiller production.

### *OsVIL2* affects tiller outgrowth

Axillary tillers are produced by two steps. The first involves formation of axillary buds and the second involves outgrowth of the axillary buds (Wai et al., 2017). To investigate whether the phenotype of fewer tillers in *osvil2* resulted from defects in bud formation or outgrowth, we examined longitudinal sections of the basal parts of the seedlings. At 14 DAG, both the WT and *osvil2-1* seedlings developed AM together with several foliage leaves and prophylls at the axils (Figs. 2A and 2B). At 28 DAG, by which time the WT had actively developed tillers, the mutant had not produced a tiller, although *osvil2-1* mutants generated axillary buds similar to WT (Figs. 2C and 2D). These results indicated that *osvil2* mutants developed axillary buds normally, but these buds failed to grow out to form tillers.

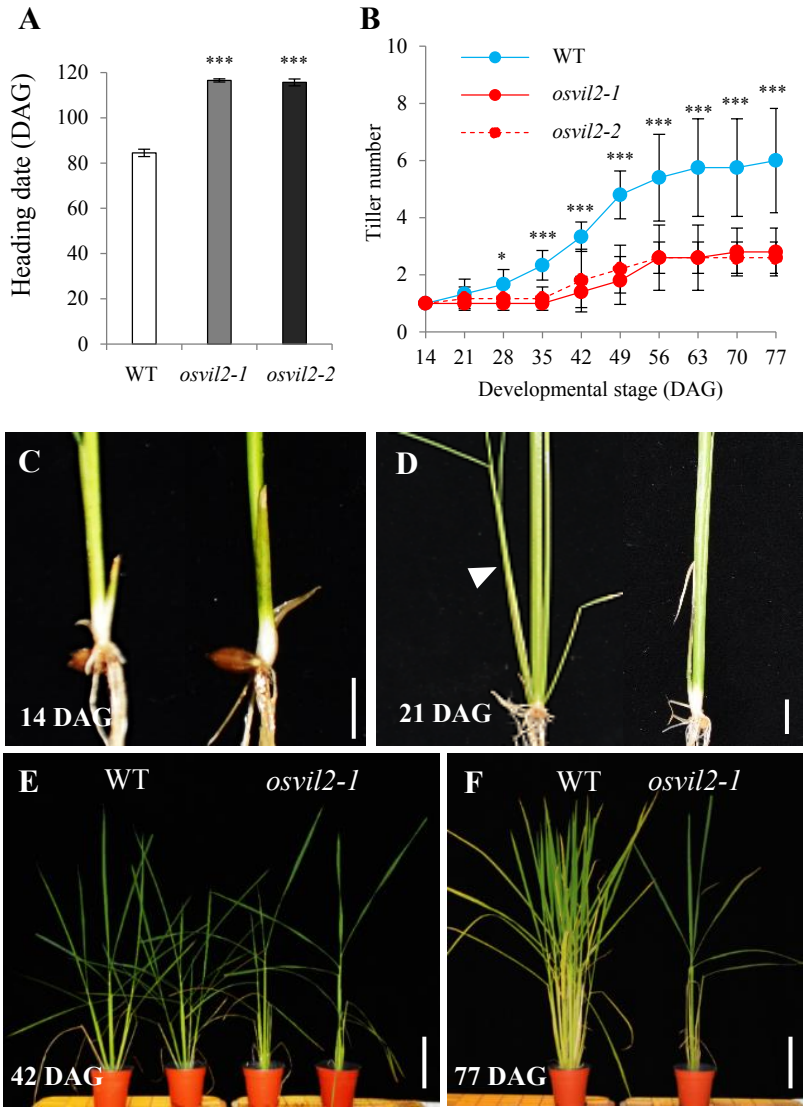


**Fig. 1. Flowering time and tiller phenotypes of WT and *osvil2* mutants.** (A) Days to heading in WT, *osvil2-1* and *osvil2-2* mutants under long-day condition (14-h light/10-h dark). The date at which the first panicles emerged were scored as the number of DAG to heading date. Error bars are SD (n = 6). (B) Number of tiller at different developmental stages. Error bars are SD (n = 6). (C-F) Tiller production by the WT and the *osvil2* mutant was monitored at 14 DAG (C), 21 DAG (D), 42 DAG (E), and 77 DAG (F). Arrowhead indicates a tiller. Scale bars = 1 cm (C and D) or 10 cm (E and F). Error bars are SD (n = 10). Statistical significance is indicated by $*P < 0.05$ and $***P < 0.001$.

### *OsVIL2* is preferentially expressed in the apical meristem

Using transgenic plants expressing the *GUS* reporter gene under the control of the *OsVIL2* promoter, we had previously observed that *OsVIL2* is strongly expressed in leaves and preferentially at the basal parts of spikelets (Yoon et al., 2018). In the present study, we found that the gene was specifically expressed at the basal part of the seedlings, especially in axillary buds and vascular tissues (Fig. 3A). To further study the expression pattern of *OsVIL2* in the meristematic regions, we performed *in situ* RNA hybridization studies using the basal parts of seedlings at 20 DAG (Figs. 3B-3F). The experiments showed that *OsVIL2* transcripts preferentially accumulated in the AM region (Figs. 3B and 3E) as well as in the axillary bud and surrounding young leaves (Figs. 3C and 3F).

### OsVIL2 affects the *OsTB1*-dependent pathway of tiller outgrowth

To investigate the genes that were affected by *osvil2* mutation, we examined expression levels of genes related to tiller development at 13 and 14 DAG when tiller outgrow did not start yet. RT-qPCR analyses of AM development pathway genes in the basal parts of culm tissues showed that the transcripts levels of *CKX2*, *OSH1*, *LAX1*, *MOC1*, *CUC1*, and *RFL1* were not significantly changed in *osvil2-1* (Supplementary Fig. S1) and *osvil2-2* (Supplementary Fig. S2) null mutants. We also examined expression patterns of tiller outgrowth-re-

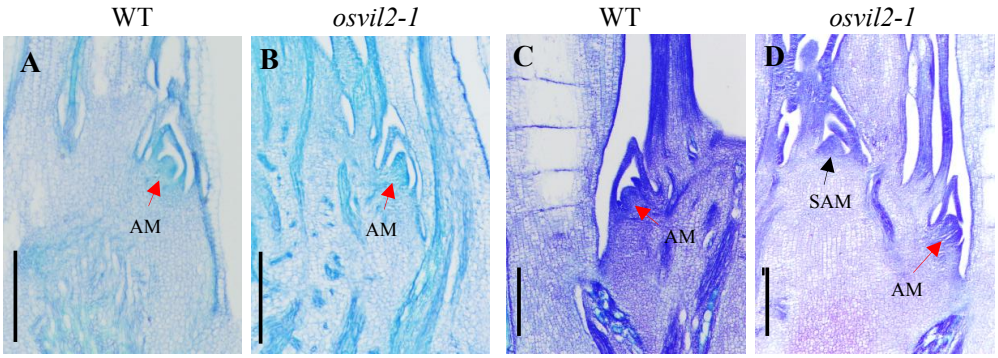


**Fig. 2. Axillary bud development in the WT and the *vil2* mutant.** (A and B) Longitudinal sections of the basal parts of rice seedlings in the WT (A) and the *osvil2-1* mutant (B) at 14 DAG. (C and D) Longitudinal sections of the basal parts of rice seedlings in the WT (C) and the *osvil2-1* mutant (D) at 28 DAG. Scale bars = 500 μm. Red arrows indicate axillary bud AM. Black arrow indicates SAM.

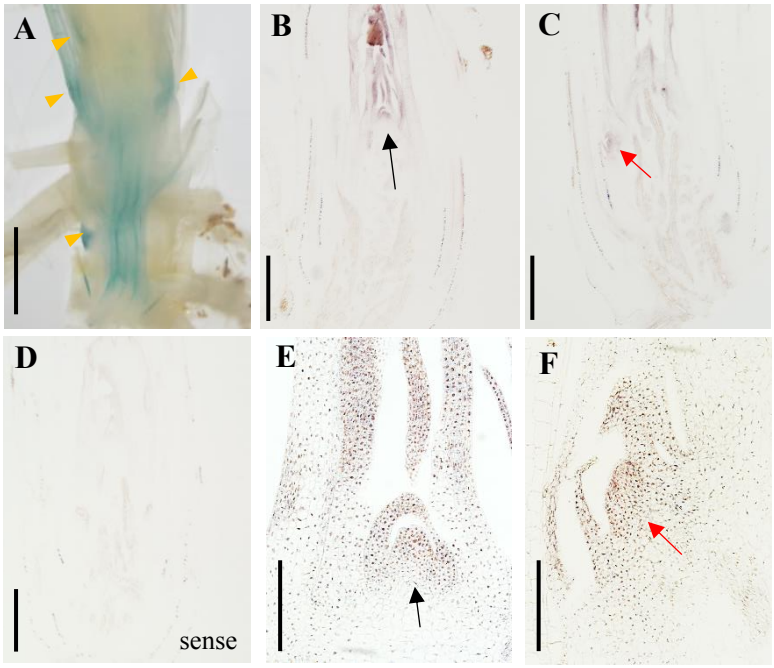


**Fig. 3. Expression patterns of *OsVIL2* in the basal parts at seedling stages.** (A) Expression patterns of *OsVIL2* promoter-*GUS* transgenic plants in the basal region of rice seedlings at 24 DAG. Arrowheads indicate axillary buds. Scale bars = 0.5 cm. (B and C) *In situ* RNA hybridization of *OsVIL2* in the basal parts of WT seedlings at 20 DAG. Scale bars = 500 μm. (D) Control experiment with a sense probe of *OsVIL2*. Scale bars = 500 μm. (E and F) Enlarged images of shoot apical region (E) and axillary bud region (F). Scale bars = 100 μm. Black arrows indicate SAM and red arrows indicate axillary buds.

lated genes. Auxin-related genes *IAA7*, *IAA20*, *PIN1*, and *PIN3* were not significantly altered in the basal parts of culm tissues of the mutant plants (Supplementary Figs. S1 and S2). However, *D10* that encodes a biosynthetic enzyme for SL was significantly suppressed in *osvil2* mutants (Supplementary Figs. S1L and S2L). Other SL-related genes and tiller outgrowth genes were not changed. These observations indicate that *OsVIL2* does not affect most of the tiller-related genes at the stage of axillary bud initiation.

We investigated the expression patterns of genes involved in tiller development in the basal parts of culm tissues at 28 and 30 DAG, at which time point axillary tillers had developed in WT but not in the *osvil2* mutant. Expression of the genes controlling axillary bud formation, namely *OSH1*, *LAX1*, *MOC1*, *CUC1*, and *RFL1*, were not significantly different between *osvil2* null mutants and the WT (Figs. 4B-4F, Supplementary Figs. S3B-S3F). This result was expected because there was no difference in axillary bud formation between *osvil2* mutants and WT.

We then studied the genes controlling axillary bud out-

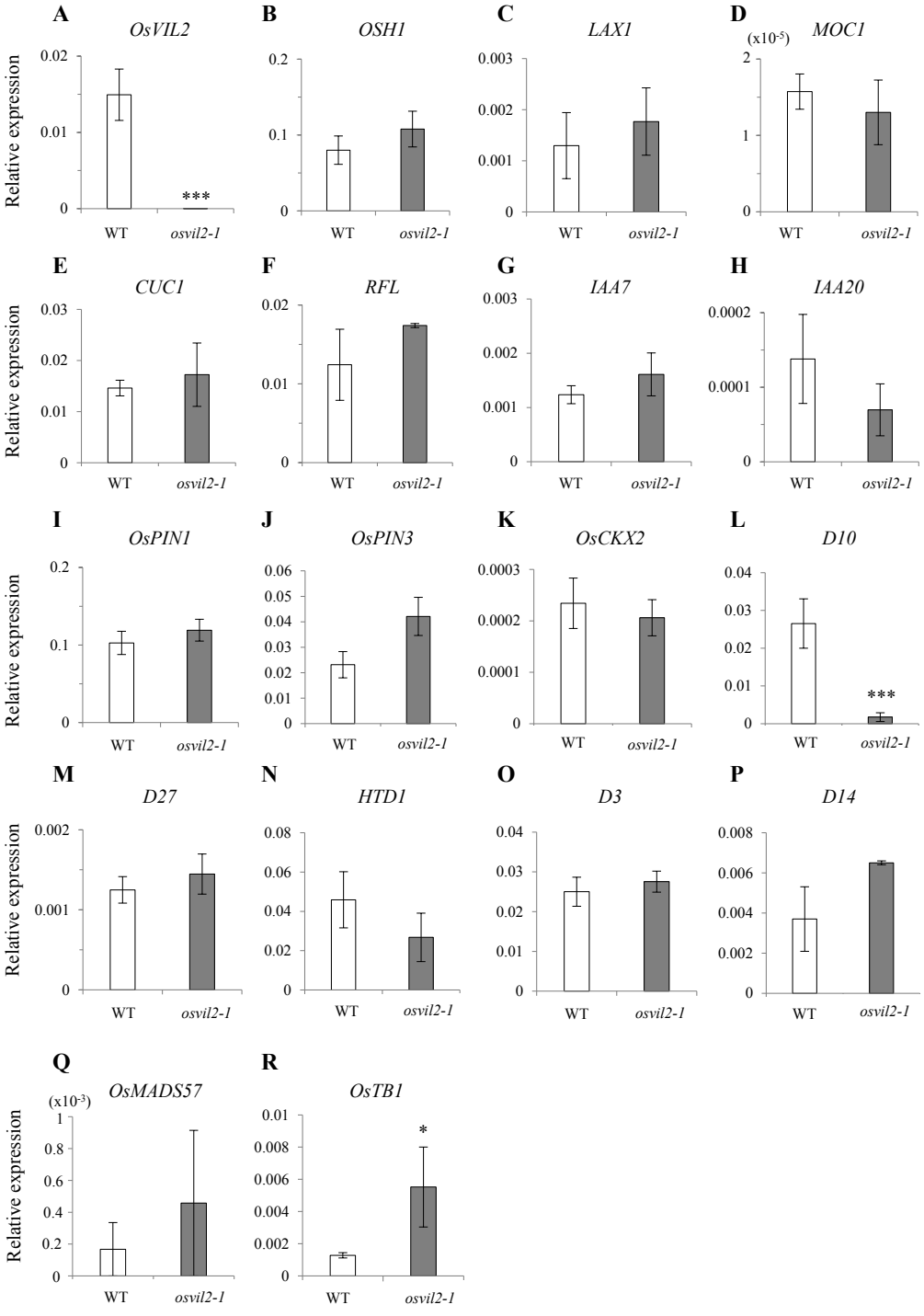


**Fig. 4. Expression levels of genes that control tiller development at 28 DAG.** (A) Transcript levels of *OsVIL2* in WT and *osvil2-1* mutant plants. (B-F) Transcript levels of axillary bud formation genes: *OSH1* (B), *LAX1* (C), *MOC1* (D), *CUC1* (E), and *RFL* (F). (G-R) Transcript levels of axillary bud outgrowth genes: *IAA7* (G), *IAA20* (H), *OsPIN1* (I), *OsPIN3* (J), *OsCKX2* (K), *D10* (L), *D27* (M), *HTD1* (N), *D3* (O), *D14* (P), *OsMADS57* (Q), and *OsTB1* (R). Error bars are SD (n = 4). Statistical significance is indicated by $*P < 0.05$ and $***P < 0.001$.

growth. Tiller bud outgrowth is controlled by hormones such as auxins, cytokinins, and SLs. Expression levels of auxin-related genes *IAA7*, *IAA20*, *PIN1*, and *PIN3*, that are involved in tiller outgrowth, were not significantly altered in *osvil2* mutants compared to the WT (Figs. 4G-4J). Expression level of the *OsCKX2* gene, encoding an enzyme catabolizing active cytokinins, was not altered (Figs. 4K). These results suggested that OsVIL2 may not be involved with auxins or cytokinins.

However, expression of *D10*, encoding a biosynthesis enzyme for SLs, was markedly down-regulated in the *osvil2* mutants (Fig. 4L, Supplementary Fig. S3L). Expression levels of additional SL-biosynthesis genes, *D27* and *HTD1*, as well as SL-signaling genes *D3* and *D14* were not significantly altered in the mutant (Figs. 4M-4P).

We also analyzed expression levels of transcription factors that control axillary bud outgrowth. Expression of a MADS-box gene *OsMADS57*, that encodes a positive regulator of axillary bud growth, was not significantly affected by the *osvil2* mutation (Fig. 4Q). However, the expression level of another transcription factor gene, *OsTB1*, was much higher in the mutants than in the WT (Fig. 4R, Supplementary Fig. S4R). Because OsTB1 is a major regulator that inhibits tiller bud outgrowth (Takeda et al., 2003), the reduced tiller outgrowth phenotype in the *osvil2* mutants is probably due to the altered expression of *OsTB1*.

To study the expression patterns of *OsTB1* during tiller development, we collected basal parts of culms from the WT and the *osvil2* mutant at 4-day intervals starting at 12 DAG (Fig. 5). Analysis of the samples showed that the expression level of *OsTB1* was gradually reduced over time in the WT, approaching almost undetectable levels at 24 DAG. However, the transcript level did not decrease in *osvil2* mutants at 24 DAG but gradually increased at the later stages (Fig. 5B). This observation supports the concept that *OsVIL2* is an inhibitor of *OsTB1*.

### OsVIL2 mediates tiller outgrowth by enrichment of H3K27me3 in *OsTB1* chromatin

Previous studies suggest that OsVIL2 interacts with PRC2 to repress target chromatins by regulating H3K27me3. The analysis of expression patterns of tiller outgrowth genes revealed that *OsTB1* is a potential target of OsVIL2. To investigate whether OsVIL2 directly repressed *OsTB1* through controlling histone modification, we measured H3K27me3 levels of *OsTB1* using the ChIP assay, with the aid of H3K27me3 antibodies in *osvil2-1* and *osvil2-2* mutants (Fig. 6). The assay showed that the 5' regulatory regions (P2, P3) of *OsTB1* chromatin were enriched in the WT, but this enrichment was not observed in the *osvil2* mutants (Figs. 6C and 6E). As a negative control, *Hd3a* chromatin was analyzed, which did not show any enrichment (Figs. 6D and 6F).

To confirm that OsVIL2 directly binds to *OsTB1* chromatin, we used OsVIL2-Myc epitope-tagged transgenic lines. As control, we used transgenic plants expressing Myc alone. The ChIP assay showed that the 5' regulatory regions (P1, P2, and P3) of *OsTB1* chromatin were enriched by Myc antibodies in the OsVIL2-Myc epitope-tagged transgenic lines (Fig. 6G) while the Myc control plants did not show the enrichment (Fig. 6H). These results suggest that the OVIL2-PRC2 complex directly binds to the *OsTB1* chromatin, thereby promoting outgrowth of tiller buds.

### *OsVIL2* induces tiller outgrowth by regulating *OsTB1* expression

To obtain a genetic relationship between *OsVIL2* and *OsTB1*, we generated *osvil2 ostb1* double mutant by CRISPR/Cas9 multiplex editing capability with the endogenous tRNA-processing system (Figs. 7A-7D). For this construction we used polycistronic tRNA-gRNA (PTG)/Cas9 method for simultaneously targeting multiple sites (Fig. 7B). We also generated *ostb1* null mutant (Supplementary Fig. S4).

At heading stage in the paddy field, *osvil2-1* mutant plants had 4 tillers per plant that is much smaller number compared to 33 of WT (Figs. 7E and 7F). On the contrary, tiller number of *ostb1* was 48.6, more than that of WT. The double mutant *osvil2 ostb1* showed the phenotypes similar to *ostb1* single mutant, having 30 tiller per plant (Figs. 7E and 7F). This experiment suggests that *OsVIL2* epistatic to *OsTB1*.

## DISCUSSION

### OsVIL2 is required for outgrowth of tiller buds

In this study, we provided evidence that OsVIL2 promotes tiller outgrowth by suppressing expression of *OsTB1*, which is an integrator of multiple pathways for tillering (Hussien et al., 2014). For instance, *OsTB1* is inhibited by cytokinins and

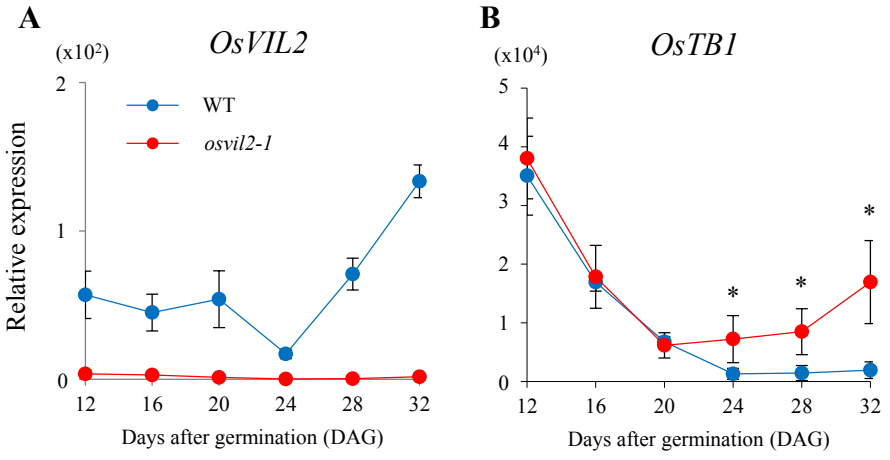


**Fig. 5. Temporal expression patterns of *OsVIL2* and *OsTB1*.** Expression levels of *OsVIL2* (A) and *OsTB1* (B) in the basal regions of WT and *osvil2* rice seedlings between 12 and 32 DAG. Error bars are SD (n = 4). Statistical significance is indicated by $*P < 0.05$.

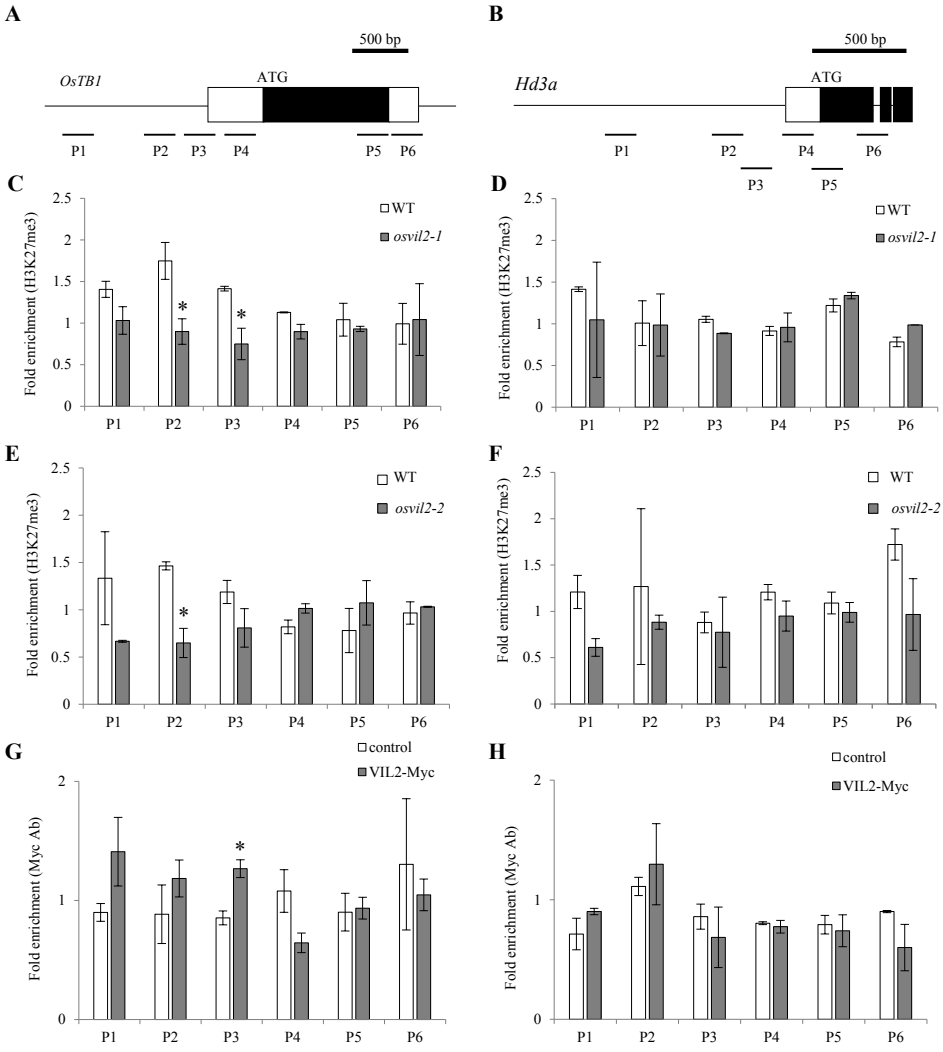


**Fig. 6. Chromatin immunoprecipitation assay.** (A) Genome structure of *OsTB1*. (B) Genome structure of *OsTB1*. (C) Analysis of H3K27me3 level on *OsTB1* chromatin in WT (white) and *osvil2-1* mutant (gray). (D) Analysis of H3K27me3 level on *Hd3a* chromatin in WT (white) and *osvil2-1* mutant (gray) using antibodies against H3K27me3. (E) Analysis of H3K27me3 level on *OsTB1* chromatin in WT (white) and *osvil2-2* mutant (gray). (F) Analysis of H3K27me3 level on *Hd3a* chromatin in WT (white) and *osvil2-2* mutant (gray) using antibodies against H3K27me3. (G) ChIP analysis of OsVIL2 enrichment on *OsTB1* chromatin. OsVIL2–Myc epitope–tagged transgenic lines were used to detect the enrichment. As a control, we used transgenic plants expressing Myc alone. (H) ChIP analysis of OsVIL2 enrichment on *Hd3a* chromatin. Plants were sampled at 28 DAG for the ChIP assay. For normalization, we used the fold enrichment method. Error bars are SD (n = 2). Statistical significance is indicated by $*P < 0.05$.

induced by auxins, whereas GAs also influence *OsTB1* (Hussien et al., 2014). However, epigenetic regulation of *OsTB1* has not previously been reported. We have previously shown that a chromatin-remodeling factor, OsVIL2, associates with H3K27me3 at the target genes to achieve suppression of expression of the target genes (Bemer and Grossniklaus, 2012; Yang et al., 2013). Our ChIP assay indicated that *OsTB1* is a potential target of OsVIL2 for tiller outgrowth.

### The expression of *D10* is significantly down-regulated in *osvil2* mutants

We observed that the expression level of *D10* was reduced in *osvil2* mutants. Because *D10* is a gene involved in SL biosynthesis, suppression of *D10* expression should result in reduced levels of SLs and should increase tiller number. However, tiller number was reduced in the *D10* mutant. This unexpected result may be due to feedback regulation of the SL biosynthesis gene. Suppression of tiller development would inhibit production of SLs, which are major inhibitors of tiller development. *D10* encodes a carotenoid cleavage dioxygenase that plays a key role in SL biosynthesis (Arite et al., 2007). Alternatively, reduction of tiller number might stimulate cytokinin signaling or inhibit auxin signaling that function upstream of *D10* (Zhang et al., 2010).

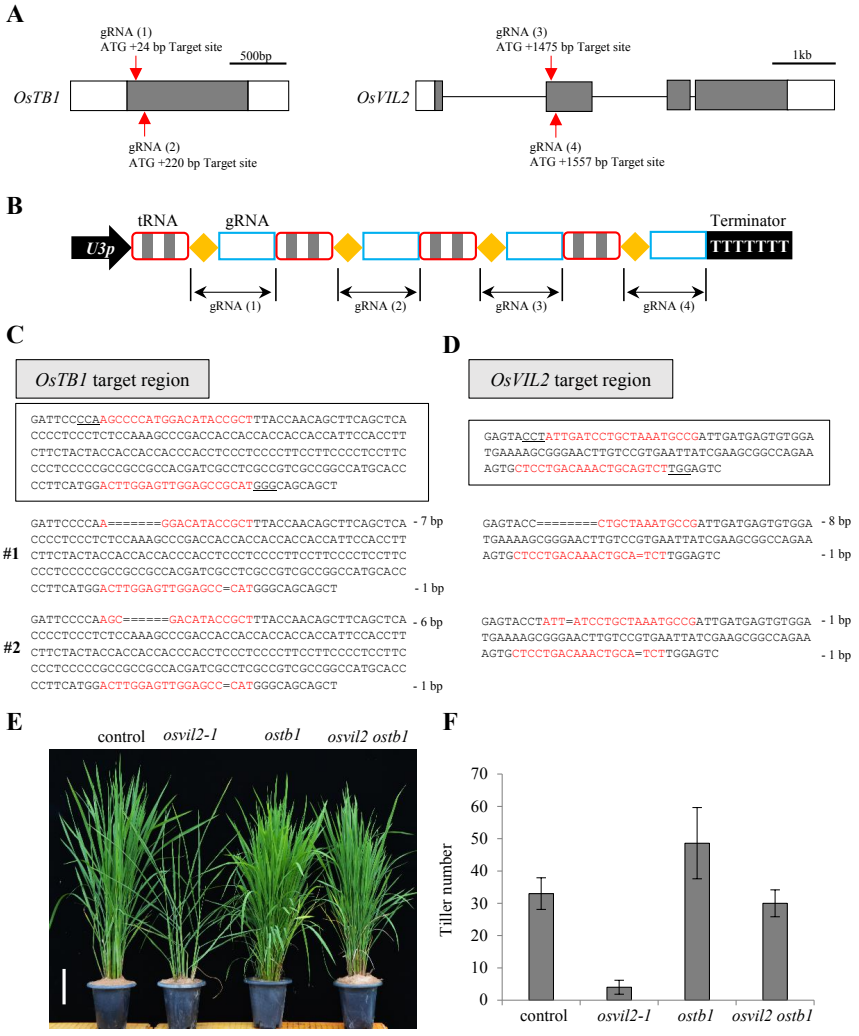


**Fig. 7. Analysis of *vil2 tb1* double mutant.** (A) Schematic diagrams of *OsTB1* (left) and *OsVIL2* (right) genes. The positions of mutation target sites are indicated with arrows. (B) Schematic diagram of the polycistronic tRNA-gRNA (PTG)/Cas9 vector for targeting multiple sites. The synthetic PTG consists of tandemly arrayed tRNA-gRNA units. (C) Mutated sites in *OsTB1*. Target sequences are indicated in red. Deleted sequences are indicated by =. (D) Mutated sites in *OsVIL2*. Target sequences are indicated in red. Deleted sequences are indicated by =. (E) Tiller phenotypes of *osvil2-1*, *ostb1*, and *osvil2 ostb1* double mutants. As a control, we generated transgenic plants with pRGEB32 empty vector. Phenotypes were observed immediately before heading stages. Scale bars = 10 cm. (F) Number of tiller in control, *osvil2-1*, *ostb1*, and *osvil2 ostb1* double mutant. Error bars are SD (n = 6).

## OsVIL2 binds to the PRC2 complex

The PRC2 complex plays important roles in the development of plants and animals by suppressing target gene expression through histone modification (Jeong et al., 2015). OsVIL2 is highly homologous to *Arabidopsis* VIN3 and VIN3-like genes that contain conserved motifs of the PHD finger, FNIII and VID domains (Greb et al., 2007). The FNIII domain of OsVIL2 binds to EMF2b, which is a component of the PRC2 complex (Yang et al., 2013). Loss-of-function mutations of *EMF2b* result in late flowering and abnormal floral organ development, which are phenotypes similar to those observed from the *osvil2* mutant (Conrad et al., 2014; Yang et al., 2013). It will be necessary to carry out further experiments to determine whether EMF2b also plays a role in tiller outgrowth and shoot branching.

## Tillering ceases at the floral transition stage

We showed that new tillers were developed during the vegetative phase and that tiller development stopped at the floral transition stage. In most late-flowering mutants that have a longer vegetative period than the WT, tiller numbers were higher than in the WT, due probably to increased vegetative growth. It is also possible that the floral transition signal directly inhibits a major regulatory gene that controls tiller bud growth. Alternatively, floral signals could affect biosynthesis of or signaling by the hormones that control tiller development. Interestingly, the *osvil2* mutant exhibited fewer tillers than did the WT, even though the mutant flowered later

than the WT. We postulate that OsVIL2 directly promotes axillary bud growth, whereas other flowering genes influence tiller number indirectly by the action of florigens.

*Note: Supplementary information is available on the Molecules and Cells website (www.molcells.org).*

### Disclosure

The authors have no potential conflicts of interest to disclose.

## ACKNOWLEDGMENTS

This work was supported in part by a grant from the Next Generation BioGreen 21 Program (Plant Molecular Breeding Center; No. PJ013210), Rural Development Administration, Republic of Korea to GA and by the Republic of Korea Basic Research Promotion Fund to JY (grant No. NRF-2018R1A6A3A11047894).

## ORCID

Jinmi Yoon https://orcid.org/0000-0003-2882-6878
Lae-Hyeon Cho https://orcid.org/0000-0003-4514-4107
Sichul Lee https://orcid.org/0000-0001-9290-2500
Richa Pasriga https://orcid.org/0000-0001-9702-7696
Win Tun https://orcid.org/0000-0001-9957-364X
Jungil Yang https://orcid.org/0000-0002-0110-6910
Hyeryung Yoon https://orcid.org/0000-0003-2546-2087
Hee Joong Jeong https://orcid.org/0000-0002-9139-7677
Jong-Seong Jeon https://orcid.org/0000-0001-6221-4993
Gynheung An https://orcid.org/0000-0002-8570-7587

## REFERENCES

Arite, T., Iwata, H., Ohshima, K., Maekawa, M., Nakajima, M., Kojima, M., Sakakibara, H., and Kyozuka J. (2007). DWARF10, an RMS1/MAX4/DAD1 ortholog, controls lateral bud outgrowth in rice. Plant J. *51*, 1019-1029.

Bemer, M. and Grossniklaus, U. (2012). Dynamic regulation of Polycomb groub activity during plant development. Curr. Opin. Plant Biol. *15*, 523-529.

Chen, Y., Fan, X., Song, W., Zhang, Y., and Xu, G. (2012). Over-expression of *OsPIN2* leads to increased tiller numbers, angle and shorter plant height through suppression of *OsLAZY1*. Plant Biotechnol. J. *10*, 139-149.

Cho, L.H., Pasriga, R., Yoon, J., Jeon, J.S., and An, G. (2018a). Roles of sugars in controlling flowering time. J. Plant Biol. *61*, 121-113.

Cho, L.H., Yoon, J., Pasriga, R., and An, G. (2016). Homodimerization of Ehd1 is required to induce flowering in rice. Plant Physiol. *170*, 2159-2171.

Cho, L.H., Yoon, J., Wai, A.H., and An, G. (2018b). *Histone deacetylase 701 (HDT701)* induces flowering in rice by modulating expression of *OsIDS1*. Mol. Cells *41*, 665-675.

Cohen, Y. and Cohen, J.Y. (2008). Analysis of variance. In Statistics and Data with R: An Applied Approach through Examples, Y. Cohen and J.Y. Cohen, eds. (Chichester: John Willey & Sons), pp. 417-461.

Conrad, L.J., Khanday, I., Johnson, C., Guiderdoni, E., An, G., Vijayraghavan, U., and Sundaresan, V. (2014). The polycomb groub gene *EMF2B* is essential for maintenance of floral meristem determinacy in rice. Plant J. *80*, 883-894.

Deshpande, G.M., Ramakrishna, K., Chongloi, G.L., and Vijayraghavan, U. (2015). Functions for rice RFL in vegetative axillary meristem specification and outgrowth. J. Exp. Bot. *66*, 2773-2784.

Greb, T., Mylne, J.S., Crevillen, P., Geraldo, N., An, H., Gendall, A.R., and Dean, C. (2007). The PHD finger protein VRN5 functions in the epigenetic silencing of *Arabidopsis FLC*. Curr. Biol. *17*, 73-78.

Guo, S., Xu, Y., Lie, H., Mao, Z., Zhang, C., Ma, Y., Zhang, Q., Meng, Z., and Chong, K. (2013). The interaction between OsMADS57 and OsTB1 modulates rice tillering via *DWARF14*. Nat. Commun. *4*, 1566.

Haring, M., Offermann, S., Danker, T., Horst, I., Peterhansel, C., and Stam, M. (2007). Chromatin immunoprecipitation: optimization, quantitative analysis and data normalization. Plant Methods *3*, 1-16.

Hussien, A., Tavakol, E., Horner, D.S., Muñoz-Amatriaín, M., Muehlbauer, G.J., and Rossini, L. (2014). Genetics of tillering in rice and barley. Plant Genome *7*, 1-20.

Ishikawa, S., Maekawa, M., Arite, T., Onishi, K., Takamure, I., and Junko, K. (2005). Suppression of tiller bud activity in tillering dwarf mutants of rice. Plant Cell Physiol. *46*, 79-86.

Jeon, J.S., Lee, S., Jung, K.H., Jun, S.H., Jeong, D.H., Lee, J., King, C., Jang, S., Lee, S., Yang, K., et al. (2000). T-DNA insertional mutagenesis for functional genomics in rice. Plant J. *22*, 561-570.

Jeong, D.H., An, S., Kang, H.G., Moon, S., Han, J.J., Park, S., Lee, H., An, K., and An, G. (2002). T-DNA insertional mutagenesis for activation tagging in rice. Plant Physiol. *130*, 1636-1644.

Jeong, H.J., Yang, J., Yi, J., and An, G. (2015). Controlling flowering time by histone methylation and acetylation in Arabidopsis and rice. J. Plant Biol. *58*, 203-210.

Jiang, L., Liu, X., Xiong, G., Liu, H., Chen, F., Wang, L., Meng, X., Liu, G., Yu, H., Yuan, Y., et al. (2013). DWARF53 acts as a repressor of strigolactone signaling in rice. Nature *504*, 401-405.

Lee, D.Y. and An, G. (2012). Two AP2 family genes, *supernumerary bract* (*SNB*) and *Osindeterminate spikelet 1* (*OsIDS1*), synergistically control inflorescence architecture and floral meristem establishment in rice. Plant J. *69*, 445-461.

Lee, D.Y., Lee, J., Moon, S., Park, S.Y., and An, G. (2007). The rice heterochronic gene *SUPERNUMERARY BRACT* regulates the transition from spikelet meristem to floral meristem. Plant J. *49*, 64-78.

Li, X., Qian, Q., Fu, Z., Wang, Y., Xiong, G., Zeng, D., Wang, X., Liu, X., Teng, S., Hiroshi, F., et al. (2003). Control of tillering in rice. Nature *422*, 618-621.

Lin, H., Wang, R., Qian, Q., Yan, M., Meng, X., Fu, Z., Yan, C., Jiang, B., Su, Z., Li, J., et al. (2009). DWARF*27*, an iron-containing protein required for the biosynthesis of strigolactones, requires rice tiller bud outgrowth. Plant Cell *21*, 1512-1525.

Minakuchi, K., Kameoka, H., Yasuno, N., Umehara, M., Luo, L., Kobayashi, K., Hanada, A., Ueno, K., Asami, T., Yamaguchi, S., et al. (2010). *FINE CULM1* (*FC1*) works downstream of strigolactones to inhibit the outgrowth of axillary buds in rice. Plant Cell Physiol. *51*, 1127-1135.

Mozgova, I. and Henning, L. (2015). The polycomb group protein regulatory network. Annu. Rev. Plant Biol. *66*, 269-296.

Nakamura, H., Xue, Y.L., Miyakawa, T., Hou, F., Qin, H.M., Fukui, K., Shi, X., Ito, E., Ito, S., and Park, S.H. (2013). Molecular mechanism of strigolactone perception by DWARF14. Nat. Commun. *4*, 2613.

Oikawa, T. and Kyozuka, J. (2009). Two-step regulation of *LAX PANICLE1* protein accumulation in axillary meristem formation in rice. Plant Cell *21*, 1095-1108.

Tabuchi, H., Zhang, Y., Hattori, S., Omae, M., Shimizu-Sato, S., Oikawa, T., Qian, Q., Nishimura, M., Kitano, H., Xie, H., et al. (2011). *LAX PANICLE2* of rice encodes a novel nuclear protein and regulates the formation of axillary meristems. Plant Cell *23*, 3276-3287.

Takeda, T., Suwa, Y., Suzuki, M., Kitano, H., Ueguchi-Tanaka, M., Ashikari, M., Matsuoka, M., and Ueguchi, C. (2003). The *OsTB1* gene negatively regulates lateral branching in rice. Plant J. *33*, 513-520.

Tanaka, W., Ohmori, Y., Ushijima, T., Matsusaka, H., Matsushita, T., Kumamaru, T., Kawano, S., and Hirano, H.Y. (2015). Axillary meristem formation in rice requires the *WUSCHEL* ortholog *TILLERS ABSENT1*. Plant Cell *27*, 1173-1184.

Tian, C. and Jiao, Y. (2015). A systems approach to understand shoot branching. Curr. Opin. Plant Biol. *3-4*, 13-19.

Wai, A.H. and An, G. (2017). Axillary meristem initiation and bud growth in rice. J. Plant Biol. *60*, 440-451.

Wang, Y. and Li, J. (2011). Branching in rice. Curr. Opin. Plant Biol. *14*, 94-99.

Wang, Y., Sun, S., Zhu, W., Jia, K., Yang, H., and Wang, X. (2013). Strigolactone/MAX2-induced degradation of brassinosteroid transcriptional effector BES1 regulates shoot branching. Dev. Cell *27*, 681-688.

Xie, K., Minkenberg, B., and Yang, Y. (2015). Boosting CRISPR/Cas9 multiplex editing capability with the endogenous tRNA-processing system. Proc. Natl. Acad. Sci. U. S. A. *112*, 3570-3575.

Xu, M., Zhu, L., Shou, H., and Wu, P. (2005). A *PIN1* family gene, *OsPIN1*, involved in auxin-dependent adventitious root emergence and tillering in rice. Plant Cell Physiol. *46*, 1674-1681.

Yang, J., Cho, L.H., Yoon, J., Yoon, H., Wai, A.H., Hong, W.J., Han, M.H., Sakakibara, H., Liang, W., Jung, K.H., et al. (2019). Chromatin interacting factor of OsVIL2 increases biomass and rice grain yield. Plant Biotechnol. J. *17*, 178-187.

Yang, J., Lee, S., Hang, R., Kim, S.R., Lee, Y.S., Cao, X., Amasino, R., and An, G. (2013). OsVIL2 functions with PRC2 to induce flowering by repressing *OsLFL1* in rice. Plant J. *73*, 566-578.

Yeh, S.Y., Chen, H.W., Ng, C.Y., Lin, C.Y., Tseng, T.H., Li, W.H., and Ku, M.S.B. (2015). Down-regulation of *Cytokinin Oxidase 2* expression increases tiller number and improves rice yield. Rice *8*, 36.

Yoon, H., Yang, J., Liang, W., Zhang, D., and An, G. (2018). OsVIL2 regulates spikelet development by controlling regulatory genes in *Oryza sativa*. Front. Plant Sci. *9*, 102.

Yoon, J., Cho, L.H., Antt, H.W., Koh, H.J., and An, G. (2017). KNOX protein OSH15 induces grain shattering by repressing lignin biosynthesis genes. Plant Physiol. *174*, 312-325.

Yoon, J., Cho, L.H., Kim, S.L., Choi, H., Koh, H.J., and An, G. (2014). The BEL1-type homeobox gene *SH5* induces seed shattering by enhancing abscission-zone development and inhibiting lignin biosynthesis. Plant J. *79*, 717-728.

Zhang, S., Li, G., Fang, J., Chen, W., Jiang, H., Zou, J., Liu, X., Zhao, X., Li, X., Chu, C., et al. (2010). The interaction among *DWARF10*, auxin and cytokinin underlie lateral bud outgrowth in rice. J. Integr. Plant Biol. *52*, 626-638.

Zhao, J., Wang, T., Wang, M., Liu, Y., Yuan, S., Gao, Y., Yin, L., Sun, W., Peng, L., Zhang, W., et al. (2014). DWARF3 participates in an SCF complex and associates with DWARF14 to suppress rice shoot branching. Plant Cell Physiol. *55*, 1096-1109.

Zou, J., Zhang, S., Zhang, W., Li, G., Chen, Z., Zhai, W., Zhao, X., Pan, X., Xie, Q., and Zhu, L. (2006). The rice *HIGH-TILLERING DWARF1* encoding an ortholog of Arabidopsis MAX3 is required for negative regulation of the outgrowth of axillary buds. Plant J. *48*, 687-696.